Multiscale dynamics of semiflexible polymers from a universal coarse-graining procedure

Elena F. Koslover[1] and Andrew J. Spakowitz[1,2]
[1]*Chemical Engineering Department, Stanford University, Stanford, California 94305, USA*
[2]*Biophysics Program, Stanford University, Stanford, California 94305, USA*
(Received 27 September 2013; published 14 July 2014)

Simulating the dynamics of a semiflexible polymer across time and length scales that bridge the rigid and flexible regimes requires a physically sound method for generating coarse-grained representations of the polymer. Here, we study the dynamic behavior of the discrete stretchable, shearable wormlike chain model, which can be used to coarse-grain a continuous semi-elastic chain at an arbitrary discretization. We show that the dynamics of this universal model match those of the wormlike chain at length scales above the discretization length. The evolution of the stress correlation, as probed through Brownian dynamics simulations, is found to reproduce the predicted behavior in both the rigid and flexible regimes, spanning over six orders of magnitude in time scales. The coarse-graining approach employed here thus enables dynamic simulation of semiflexible polymers at lengths and times that were previously inaccessible with conventional methods.

DOI: 10.1103/PhysRevE.90.013304 PACS number(s): 05.10.−a, 87.15.H−, 36.20.Ey, 82.35.Pq

A large class of biological and synthetic polymers exhibit semiflexible properties, transitioning from rigid to flexible above a certain characteristic length scale. These polymers are generally described using a continuous wormlike chain (WLC) model [1,2] with a persistence length ℓ_p setting the scale of flexibility. Biopolymers, in particular, span a vast range of persistence lengths, from a few nanometers for single-stranded nucleic acids [3] to millimeters for microtubules [4]. Modeling the physical properties of polymer systems thus necessitates the ability to handle the full range of polymer flexibilities.

Much interest has focused on the dynamics of semiflexible polymers, including the viscoelastic properties of cytoskeletal filaments and DNA, addressed using microrheological [5,6] and single-molecule perturbation studies [7,8]. The dynamic behavior of fully flexible and fully rigid polymers is well characterized [9]. The viscoelastic scaling for semiflexible chains has been more recently measured and theoretically derived [10,11]. These scaling properties were confirmed and extended with computational studies focusing on the stiff regime [12,13].

Wormlike chain simulations are generally carried out using the bead-rod model [14], wherein the chain is discretized into a sequence of rigid segments with a quadratic bending potential. Such simulations become computationally expensive for chains much longer than a persistence length, as long length and time scales require correspondingly larger numbers of beads and time steps. While other studies have combined different fine and coarse-grained models to expand the accessible range [15], we present here a single consistent model that can systematically and efficiently reconcile all time scales associated with the dynamics of long chains.

In previous publications, we demonstrated that any locally defined polymer chain can be coarse-grained by mapping to a continuous stretchable, shearable, wormlike chain model (ssWLC) [16] or its discrete analog (dssWLC) [17]. In these models, each point along the polymer is described not only by its position in space but also by an effective orientation vector. The polymer contour tends to follow this orientation vector, with quadratic penalties for turning of the orientation, shearing of the contour away from the preferred orientation, and stretching of the contour. Our approach, based on matching components of low-order moments of the end-to-end distance, allows for the systematic generation of coarse-grained models with an arbitrary degree of discretization that could match the statistical behavior of the canonical wormlike chain above the discretization length. In this work, we demonstrate that the dssWLC model can be employed in dynamic simulations of semiflexible polymers to address previously inaccessible length and time scales by adjusting the degree of coarse-graining to access different scales. To aid in the implementation of our model, we provide computer scripts on our website [18] to determine the coarse-grained parameters for our model.

The dssWLC model is defined by a sequence of beads numbered from 0 to N, with positions $\vec{r}_i$ and a unit vector $\vec{u}_i$ attached to each bead. The energy function for a particular chain configuration is given by [17]

$$\beta E(\{\vec{R}_i,\vec{u}_i\}) = \sum_{i=1}^{N}\left[\frac{\epsilon_b}{2\Delta}|\vec{u}_i-\vec{u}_{i-1}-\eta\vec{R}_i^{\perp}|^2 + \frac{\epsilon_\parallel}{2\Delta}(\vec{R}_i\cdot\vec{u}_{i-1}-\Delta\gamma)^2+\frac{\epsilon_\perp}{2\Delta}|\vec{R}_i^{\perp}|^2\right], \quad (1)$$

where $\beta = 1/(k_BT)$, k_B is the Boltzmann constant, $\vec{R}_i = \vec{r}_i - \vec{r}_{i-1}$, and $\vec{R}_i^{\perp} = \vec{R}_i - (\vec{R}_i\cdot\vec{u}_{i-1})\vec{u}_{i-1}$. Each segment of this discrete model represents a continuous polymer contour length of Δ. The model parameters include the bend modulus ϵ_b, stretch modulus $\epsilon_\parallel$, shear modulus $\epsilon_\perp$, fractional ground-state length γ, and bend-shear coupling η. These parameters can be found for a wormlike chain with persistence length ℓ_p at any discretization length Δ, as described in our previous work [17].

For short discretization lengths $\Delta \ll \ell_p$, the bend and shear moduli become very stiff, and the interbead separations tend to align along the orientation vectors ($\vec{R}_i \to \Delta\vec{u}_i$) as the discrete chain more closely approximates the continuous WLC. With segments increasingly coarse-grained up to a discretization of $\Delta = \ell_p$, the bend and shear moduli as well as the fractional ground-state length of a segment γ decrease as thermal

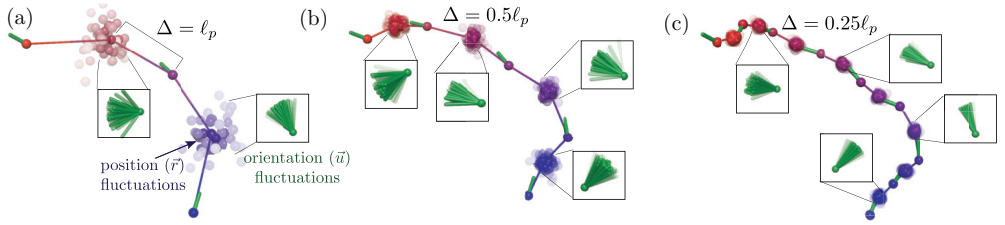

FIG. 1. (Color) Position and orientation fluctuations in the dssWLC model with discretization lengths (a) $\Delta = \ell_p$, (b) $\Delta = 0.5\ell_p$, and (c) $\Delta = 0.25\ell_p$, indicating the increased flexibility for more coarse-grained discretizations. Chain configurations are shown with every other bead position and orientation fixed, while the remaining positions and orientations are sampled from the appropriate distribution. Transparency of the beads is proportional to the partition function at that position, integrated over all $\vec{u}$. Insets show distributions of orientation vectors $\vec{u}$ integrated over all possible bead positions.

fluctuations within the length scale of Δ are incorporated into the model (illustrated in Fig. 1). The model can be further applied to arbitrarily large discretizations, as described in previous work [17].

Using our dssWLC model in dynamic simulations requires both a verification that the model recapitulates the known relaxation behavior of the WLC model as well as a procedure for determining the dynamic simulation parameters. To explore the dynamic behavior of this model, we begin by studying its continuous analog [16], which can be obtained by replacing the summation in Eq. (1) with an integral over the chain contour s from 0 to L, replacing $(\vec{u}_i - \vec{u}_{i-1})/\Delta$ with $\partial_s \vec{u}$ and $\vec{R}_i/\Delta$ with $\partial_s \vec{r}$.

We model the dynamic relaxation of the ssWLC near its ground state by deriving and solving the relevant equations of motion. We introduce an orthogonal triad of unit vectors at each point along the chain $\vec{e}_1(s), \vec{e}_2(s), \vec{e}_3(s) = \vec{u}(s)$ and define the coordinates $X_i = \vec{r}_s \cdot \vec{e}_i$ for $i = 1,2$, representing the local shear of the chain, $X_3 = \vec{r}_s \cdot \vec{e}_3 - \gamma$ giving the local stretch, and Ω_i representing the curvature such that $\partial_s \vec{e}_i = \boldsymbol{\Omega} \times \vec{e}_i$. Near the ground state, X_i and Ω_i should be small, so we include only the lowest-order terms in our equations.

We begin with the deterministic dynamic equations for a ssWLC under the free-draining approximation

$$\zeta_r \frac{d\vec{r}}{dt} = -\frac{\delta E}{\delta \vec{r}}, \tag{2}$$

$$\zeta_u \frac{d\vec{u}}{dt} = -\frac{\delta E}{\delta \vec{u}} + \Lambda \vec{u}, \tag{3}$$

where ζ_r and ζ_u give the friction coefficients per unit length for the chain position and orientation vectors, respectively. The final term represents a tension force set to enforce the constraint $\frac{d\vec{u}}{dt} \cdot \vec{u} = 0$, which maintains the vectors $\vec{u}$ to be of unit magnitude. Re-expressing in terms of our newly defined coordinates, in a manner analogous to the parallel development for the canonical wormlike chain [19], yields the following set of linearized dynamic equations:

$$\frac{dX_1}{dt} = \frac{1}{\zeta_r}[-\eta\epsilon_b\Omega_{2ss} + \hat{\epsilon}_\perp X_{1ss}] + \frac{\gamma}{\zeta_u}[-\gamma\hat{\epsilon}_\perp X_1 - \epsilon_b\Omega_{2s} + \eta\epsilon_b X_{1s} + \eta\epsilon_b\gamma\Omega_2], \tag{4}$$

$$\frac{dX_2}{dt} = \frac{1}{\zeta_r}[\eta\epsilon_b\Omega_{1ss} + \hat{\epsilon}_\perp X_{2ss}] + \frac{\gamma}{\zeta_u}[-\gamma\hat{\epsilon}_\perp X_2 + \epsilon_b\Omega_{1s} + \eta\epsilon_b X_{2s} - \eta\epsilon_b\gamma\Omega_1], \tag{5}$$

$$\frac{dX_3}{dt} = \frac{\epsilon_\parallel}{\zeta_r} X_{3ss}, \tag{6}$$

$$\frac{d\Omega_1}{dt} = \frac{1}{\zeta_u}[-\hat{\epsilon}_\perp\gamma X_{2s} + \epsilon_b\Omega_{1ss} + \eta\epsilon_b(X_{2ss} - \gamma\Omega_{1s})], \tag{7}$$

$$\frac{d\Omega_2}{dt} = \frac{1}{\zeta_u}[\hat{\epsilon}_\perp\gamma X_{1s} + \epsilon_b\Omega_{2ss} - \eta\epsilon_b(X_{1ss} + \gamma\Omega_{2s})], \tag{8}$$

where we define $\hat{\epsilon}_\perp = \epsilon_\perp + \eta^2\epsilon_b$, $X_{1s} = \partial_s X_1$, and so forth. We note that all coordinates have been defined such that they vanish in the ground-state configuration, so that for small deformations we can drop all higher-order terms in the dynamic equations to obtain the linearized forms in Eqs. (4) to (8). For free ends, the associated boundary conditions are $X_i(0) = X_i(L) = \Omega_i(0) = \Omega_i(L) = 0$. We note that the dynamics of the stretch coordinate X_3 exactly parallel those of the Rouse chain [9], while the shear and bend dynamics are coupled together. Equations (4) to (8) can be solved by decomposing each degree of freedom into normal modes $\Phi_p = \sqrt{2/L}\sin(\pi ps/L)$. The presence of first derivative terms results in dynamic coupling between different modes for the bend and shear coordinates. The coupled dynamics of X_1, Ω_2 can then be expressed as a set of linear equations whose eigenvalues determine the time scales of decay for the bend and shear modes. We analytically solve this linearized form of the model to facilitate a comparison to known results for semiflexible chains and to aid in the selection of dynamic parameters. Subsequently, we discuss simulations of the discretized model employing these parameters which can extend to nonlinear regimes so long as the discretization length scale is kept relatively small compared to the local deformation.

For the canonical WLC model with persistence length ℓ_p, the relaxation time of the most coarse-grained bending mode is given by $\tau_{\text{bend}} = \zeta_r L^4/[(3\pi/2)^4\ell_p]$ [20]. In Fig. 2, we plot the longest relaxation time versus chain length for the continuous chain limit of our dssWLC models with different discretizations. We note that for long lengths, the models all approach a universal curve that coincides with the WLC

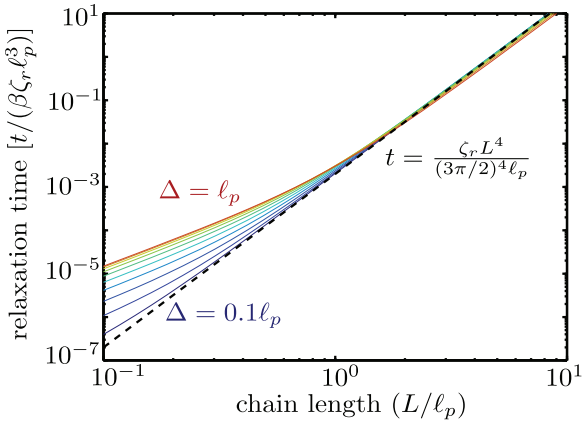

FIG. 2. (Color) Longest relaxation time for the linearized continuous analog of the dssWLC with different discretization lengths ($0.1\ell_p \leqslant \Delta \leqslant \ell_p$, in increments of $0.1\ell_p$), as a function of total chain length L. Dashed line represents the canonical WLC solution.

result [20]. Thus, the dssWLC models accurately reproduce the long length-scale dynamics of the wormlike chain.

To implement the dssWLC model in dynamic simulations, we must select an appropriate value for the friction coefficient ζ_u of the orientation vectors. This friction coefficient should be sufficiently small to not affect the dynamic behavior on length scales above a single segment. In Fig. 3, we plot the longest relaxation time for a shearable chain of length Δ as a function of ζ_u for increasingly coarse-grained values of Δ. For simulation purposes, selecting a larger friction coefficient enables larger time steps and greater computational efficiency. We thus chose ζ_u to be the cutoff value below which the relaxation time is insensitive to this friction coefficient. A tabulation of these values, as well as other model parameters, is provided on our website [18]. We note that the selected friction coefficient for each bead in a simulation [$\zeta_{ub} = \zeta_u L/(N+1)$] scales approximately as Δ^3, as expected for the rotational diffusive motion of a rigid rod [9].

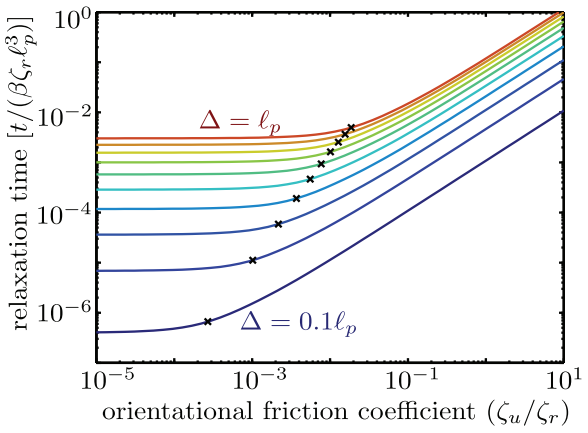

FIG. 3. (Color) Relaxation time of a single discretization length for the continuous analog of the dssWLC, as a function of the orientational friction coefficient. Black crosses correspond to the value of ζ_u selected for Brownian dynamics simulations.

We carry out a Brownian dynamics simulation of a discretized wormlike chain of length $L = 10\ell_p$ using the aforementioned procedure for determining ζ_u. The dynamics of the chain are evolved according to the overdamped Langevin equations for each bead i,

$$\zeta_{rb}\frac{d\vec{r}_i}{dt} = -\frac{\partial E}{\partial \vec{r}_i} + \vec{F}_i^{(B,r)},$$
$$\zeta_{ub}\frac{d\vec{u}_i}{dt} = -\frac{\partial E}{\partial \vec{u}_i} + \vec{F}_i^{(B,u)}, \tag{9}$$

where $\vec{F}^{(B,r)}$ and $\vec{F}^{(B,u)}$ are the Brownian forces for the bead position and orientation, selected from a normal distribution with zero mean and variance $2\zeta_{rb}/\delta t$ and $2\zeta_{ub}/\delta t$ (for discretized time step δt). To increase computational efficiency, we employ a modified fourth-order Runge-Kutta formalism to propagate the dynamic equations [21,22]. This method resolves elastic forces to fourth order while maintaining a constant Brownian force over the δt time step. In test runs of particles in harmonic wells, this method allowed δt to increase by more than an order of magnitude when elastic forces were significantly stronger than Brownian forces (see Supplemental Material) [23].

The translational friction coefficient is given by $\zeta_{rb} = \zeta_r L/(N+1)$. For the orientation vectors, only the force perpendicular to $\vec{u}$ is employed, and the vectors are normalized at each step to prevent accumulation of numerical errors. The time step is chosen as $\delta t = 0.5\zeta_{ub}/(\epsilon_\perp \gamma^2 \Delta)$. The starting configurations are selected from an equilibrium distribution.

The polymer stress tensor $\boldsymbol{\sigma} = -\sum(\vec{r}_i - \vec{r}_c)\vec{F}_i^{\text{total}}$ (where $\vec{r}_c$ is the center of mass) is calculated periodically throughout the simulation as described in previous works [13,24]. The time correlation of the shear stress, defined as $C_{\text{shear}}(t) = 1/6\sum_{i\neq j}\langle\sigma_{ij}(t)\sigma_{ij}(0)\rangle$ is used to track the dynamic behavior of the polymer [12,13]. From the fluctuation-dissipation theorem, the microscopically defined correlation function $C_{\text{shear}}(t)$ is related to the single polymer contribution of the macroscopic shear stress response function via $G(t) = -\beta dC_{\text{shear}}/dt$ [9,12]. This macroscopic response function has been previously calculated for a canonical WLC under high-frequency oscillatory stresses by assuming affine longitudinal deformation of the chain [10,11]. The resulting short-time behavior of the shear stress correlation is given by

$$C_{\text{shear}}^{\text{wlc}}(t) = \frac{(2\zeta_r)^{3/4} L \ell_p^{5/4} \beta^{-5/4}}{15\Gamma(1/4)} t^{-3/4}. \tag{10}$$

At longer times, increasingly flexible length scales begin to equilibrate. In particular, for times $t \gg \tau_p$, where $\tau_p = \zeta_r \ell_p^3/(3\pi/2)^4$ is the relaxation time for one persistence length, the dynamics of the stress relaxation should approach those of a Gaussian polymer with Kuhn length $2\ell_p$. The shear stress correlation function for such a polymer using the Rouse model is given by [9]

$$C_{\text{shear}}^{\text{rouse}}(t) = \sqrt{\frac{\zeta_r \ell_p L^2}{12\beta^3\pi}} t^{-1/2}. \tag{11}$$

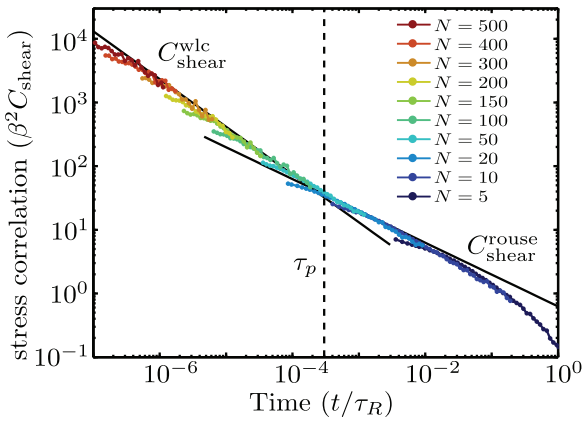

FIG. 4. (Color) Shear stress correlation function from Brownian dynamics simulations of a semiflexible chain of length $L = 10\ell_p$, using the dssWLC model with different discretization lengths $\Delta = L/N$. Solid black lines show the predicted behavior for a stiff WLC ($C^{\text{wlc}}_{\text{shear}}$) and a fully flexible Rouse chain ($C^{\text{rouse}}_{\text{shear}}$). Dashed vertical line indicates time scale of relaxation for a single persistence length τ_p.

This scaling is valid only for times $\tau_p \ll t \ll \tau_R$, where $\tau_R = 2\ell_p\zeta_r L^2/(3\pi^2\beta^3)$ is the relaxation time for the entire chain. At longer times, the shear correlation for the Rouse chain should fall off exponentially.

The decay of the shear stress correlation $C_{\text{shear}}(t)$ is plotted in Fig. 4 as calculated from a series of Brownian dynamics simulations using the dssWLC model with discretization lengths $\Delta = 0.02\ell_p$ ($N = 500$) to $\Delta = 2\ell_p$ ($N = 5$). At the shortest time scales, the dynamics of each simulated chain are dependent on the discretization length. However, at longer times, all of the simulated correlation functions fall on a universal curve that matches the predicted dynamic behavior, decaying as $C^{\text{wlc}}_{\text{shear}}$ for $t \ll \tau_p$, $C^{\text{rouse}}_{\text{shear}}$ for $\tau_p \ll t \ll \tau_R$ and showing an exponential dropoff near $t \geqslant \tau_R$.

We note that not only the scaling exponents but the exact forms of these theoretical correlation functions are matched by our simulations on time scales above those required to equilibrate individual segments. Interestingly, our results indicate that even a chain of moderate length ($L = 10\ell_p$) exhibits flexible chain dynamics at long time scales. As this behavior arises from a summation over many modes shorter than the chain length [9], this finding emphasizes the significance of bend fluctuations on lengths comparable to ℓ_p, which are excluded in studies that coarse-grain long chains using bead-rod models [13]. Overall, we demonstrate that the dssWLC model can be employed to simulate the dynamics of an intermediate length semiflexible polymer across time scales spanning six orders of magnitude, including both the rigid and flexible regimes.

Previous simulations of semiflexible polymer dynamics using the bead-rod model have been limited to very short, nearly rigid chains [12,13,25]. This limitation arises from the fact that the discretization length of such chains must be much less than the persistence length to accurately reproduce the physics of the continuous chain. Thus increasing chain length requires increasing the number of beads in the simulation. Furthermore, the relaxation time for the tension forces required to maintain constant segment lengths in such a model scales as N^{-2}, where N is the number of beads [25]. The maximal time step in a Brownian dynamics simulation must decrease accordingly to accurately reproduce the dynamics. Given that a chain length longer than ℓ_p equilibrates on a time scale of $\tau_R \sim L^2$, the computational effort required to simulate the full range of dynamic behavior in such a chain scales as L^5.

Using the dssWLC model, however, the discretization length can be extended to accommodate longer time scales, so that the entire range of dynamic behavior can be spanned by a sequence of simulations with different discretizations, as in Fig. 4. We note that for the chain length used here, limiting the discretization to $\Delta < 0.1$ as would be required if employing the bead-rod model would require increasing the number of time steps by a factor of about 10^4 to reach the terminal relaxation time. While other studies have targeted a wide range of time scales by joining together different models to represent fine and coarse-grained behavior [15,26], our model presents an alternative unified approach that can be used to span over the full range of scales while assuring the correct statistics and dynamics at long lengths.

The dssWLC model provides a versatile approach for simulating semiflexible dynamics by adjusting the discretization to suit the time and length scale of interest. Short time-scale phenomena can be modeled using fine-grained simulated chains while longer time scales can be accessed by more coarse-grained versions of the model. Efficient methods for combining different levels of coarse-graining by dynamic rediscretization within a single simulation will be addressed in future work. This approach opens up the possibility of simulating much larger systems than has previously proved feasible. Of particular interest are the dynamics of linked or entangled networks of semiflexible chains, which could in principle be simulated using a discretization scale not much smaller than the interlink separation. Potential biological applications include modeling the multiscale packaging of genomic DNA and the dynamic properties of the cytoskeleton.

In this work we focus specifically on freely draining polymer chains. In principle, hydrodynamic interactions could be included in this model using some of the same approximations that have been employed in other coarse-grained simulations [27,28]. While complications inevitably arise in representing the hydrodynamics of a coarse-grained segment, the dssWLC model can be treated analogously to other bead-spring chains in this regard.

Finally, we note that the dssWLC is not limited to discretizing the classic wormlike chain and can be employed for generating coarse-grained representations for studying the large-scale dynamics of any microscopic polymer model [17]. The model presented here thus has a wide range of applications in the field of polymer dynamics.

We are grateful for helpful discussions with Ekaterina Pilyugina, Jay Schieber, and Panagiotis Dimitrakopoulos. Funding for this project was provided by the NSF CAREER award.

[1] O. Kratky and G. Porod, Recl. Trav. Chim. Pay. B **68**, 1106 (1949).
[2] H. Yamakawa, *Helical Wormlike Chains in Polymer Solutions* (Springer, Berlin, 1997).
[3] M. Murphy, I. Rasnik, W. Cheng, T. M. Lohman, and T. Ha, Biophys. J. **86**, 2530 (2004).
[4] F. Gittes, B. Mickey, J. Nettleton, and J. Howard, J. Cell Biol. **120**, 923 (1993).
[5] F. Gittes, B. Schnurr, P. D. Olmsted, F. C. MacKintosh, and C. F. Schmidt, Phys. Rev. Lett. **79**, 3286 (1997).
[6] T. Mason, A. Dhople, and D. Wirtz, Macromolecules **31**, 3600 (1998).
[7] J.-C. Meiners and S. R. Quake, Phys. Rev. Lett. **84**, 5014 (2000).
[8] D. Riveline, C. H. Wiggins, R. E. Goldstein, and A. Ott, Phys. Rev. E **56**, R1330(R) (1997).
[9] M. Doi and S. Edwards, *The Theory of Polymer Dynamics* (Oxford University Press, New York, 1988).
[10] F. Gittes and F. C. MacKintosh, Phys. Rev. E **58**, R1241(R) (1998).
[11] D. C. Morse, Phys. Rev. E **58**, R1237 (1998).
[12] M. Pasquali, V. Shankar, and D. C. Morse, Phys. Rev. E **64**, 020802 (2001).
[13] P. Dimitrakopoulos, J. F. Brady, and Z.-G. Wang, Phys. Rev. E **64**, 050803(R) (2001).
[14] M. Somasi, B. Khomami, N. Woo, J. Hur, and E. Shaqfeh, J. Non-Newtonian Fluid Mech. **108**, 227 (2002).
[15] I. S. Dalal, A. Albaugh, N. Hoda, and R. G. Larson, Macromolecules **45**, 9493 (2012).
[16] E. F. Koslover and A. J. Spakowitz, Macromolecules **46**, 2003 (2013).
[17] E. F. Koslover and A. J. Spakowitz, Soft Matter **9**, 7016 (2013).
[18] A. J. Spakowitz, Spakowitz research group website, http://www.stanford.edu/∼ajspakow/index.html.
[19] R. E. Goldstein, T. R. Powers, and C. H. Wiggins, Phys. Rev. Lett. **80**, 5232 (1998).
[20] S. R. Aragon and R. Pecora, Macromolecules **18**, 1868 (1985).
[21] S. Mehraeen, N. Cordella, J. S. Yoo, and A. J. Spakowitz, Soft Matter **7**, 8789 (2011).
[22] S. C. Weber, J. A. Theriot, and A. J. Spakowitz, Phys. Rev. E **82**, 011913 (2010).
[23] See Supplemental Material at http://link.aps.org/supplemental/10.1103/PhysRevE.90.013304 for more information on the method used.
[24] P. Grassia and E. Hinch, J. Fluid Mech. **308**, 255 (1996).
[25] I. D. Dissanayake and P. Dimitrakopoulos, Phys. Rev. E **74**, 021918 (2006).
[26] I. S. Dalal, N. Hoda, and R. G. Larson, J. Rheol. **56**, 305 (2012).
[27] J. Magda, R. Larson, and M. Mackay, J. Chem. Phys. **89**, 2504 (1988).
[28] C.-C. Hsieh, L. Li, and R. G. Larson, J. Non-Newtonian Fluid Mech. **113**, 147 (2003).